Evaluating Hydrogeomorphic Condition Across Ecosystem States in a Non-tidal, Brackish Peat Marsh of the Florida Coastal Everglades, USA

Lukas Lamb-Wotton[1,8] · Tiffany G. Troxler[2,3] · Carlos Coronado-Molina[4] · Stephen E. Davis[5] · Daniel Gann[6] · Khandker S. Ishtiaq[3,5] · Sparkle L. Malone[7] · Paulo Olivas[2] · David T. Rudnick[8] · Fred H. Sklar[4]

Abstract

Emergent marsh and open water have been identified as alternate stable states in tidal marshes with large, relative differences in hydrogeomorphic conditions. In the Florida coastal Everglades, concern has been raised regarding the loss of non-tidal, coastal peat marsh via dieback of emergent vegetation and peat collapse. To aid in the identification of alternate stable states, our objective was to characterize the variability of hydrogeomorphic and biologic conditions using a field survey and long-term monitoring of hydrologic and geomorphic conditions across a range of vegetated (emergent, submerged) and unvegetated (open water) communities, which we refer to as "ecosystem states," in a non-tidal, brackish peat marsh of the coastal Everglades. Results show (1) linear relationships among field-surveyed geomorphic, hydrologic, and biologic variables, with a 35-cm mean difference in soil surface elevation between emergent and open water states, (2) an overall decline in soil elevation in the submerged state that was related to cumulative dry days, and (3) a 2× increase in porewater salinity during the dry season in the emergent state that was also related to the number of dry days. Coupled with findings from previous experiments, we propose a conceptual model that describes how seasonal hydrologic variability may lead to ecosystem state transitions between emergent and open water alternate states. Since vegetative states are only moderately salt tolerant, as sea-level rise pushes the saltwater front inland, the importance of continued progress on Everglades restoration projects, with an aim to increase the volume of freshwater being delivered to coastal wetlands, is the primary management intervention available to mitigate salinization and slow ecosystem state shifts in non-tidal, brackish peat marshes.

Keywords Coastal marsh · Sea-level rise · Salinization · Elevation change · Surface elevation table · Alternate stable state

Introduction

Coastal marshes, including tidal freshwater marshes, brackish non-tidal peat marshes, and salt marshes, are currently contending with increasing sea levels (Sweet et al. 2022).

Sea-level rise is accelerating saltwater intrusion into marshes that can lack the adaptive capacity to thrive in a salinized environment (Herbert et al. 2015). Salinization occurs not only through surface or subsurface saltwater intrusion from increasing sea levels, but also from declining inland freshwater flows because of water management for water supply and flood control (Dessu et al. 2018). During periods of sustained

Communicated by John C. Callaway

✉ Lukas Lamb-Wotton
  llambwotton@tulane.edu

1 Department of Earth and Environmental Sciences, Tulane University, New Orleans, LA 70118, USA

2 Department of Earth and Environment, Florida International University, Miami, FL 33199, USA

3 Institute of Environment, Sea-level Solutions Center,, Florida International University, Miami, FL 33199, USA

4 Everglades Systems Assessment, South Florida Water Management District, West Palm Beach, FL 33406, USA

5 The Everglades Foundation, Palmetto Bay, FL 33157, USA

6 Department of Biological Sciences, Florida International University, Miami, FL 33199, USA

7 School of the Environment, Yale University, New Haven, CT 06501, USA

8 South Florida Natural Resources Center, Everglades National Park, Homestead, FL 33034, USA

🍭 Springer

increases in sea level and salinization, coastal marshes can migrate laterally and replace inland marshes when sufficient space exists to accommodate their migration (Enwright et al. 2016; Osland et al. 2022). In the absence of sufficient accommodation space and without adaptive management interventions, such as thin-layer placement (Raposa et al. 2023), there is significant concern that increasing sea levels and coincident salinization will drive losses in coastal marsh extent.

Salinization can shift the marsh into a state of decline and degradation where relatively rapid, and often irreversible, transitions to an open water alternative state occur (Beisner et al. 2003). The concept of alternate stable states refers to when there are two or more states in which an ecosystem can persist within the same range of environmental conditions (Ratajczak et al. 2018). In tidal marshes, emergent marsh and open water have been identified as alternate stable states (Wang et al. 2021). These alternate states have been identified by quantifying differences in geomorphic and hydrologic conditions, including soil surface elevation and water depths, and comparing associated frequency distributions (Fagherazzi et al. 2006; van Wesenbeeck et al. 2008; Marani et al. 2013; Wang and Temmerman 2013; Moffett et al. 2015; Schepers et al. 2020; Stagg et al. 2021; Cadigan et al. 2022). It has been shown that this conversion from emergent marsh to open water across coastal marshes can be an irreversible, hysteretic process due to large differences in relative elevation that increase the depth and duration of inundation and prevent revegetation (Chambers et al. 2019; Wang et al. 2021). The identification and characterization of alternate states can therefore alert water managers about the potential loss of emergent marsh.

In the Florida Everglades, both freshwater and marine processes influence coastal landscape composition and configuration (Childers et al. 2019). Over the last century, significant anthropogenic modifications have occurred across the Florida Everglades that drastically altered the volume, timing, and distribution of freshwater delivered to the coastal landscape and prompting the largest freshwater restoration effort in the world (McVoy et al. 2011; Sklar et al. 2019). Since the Everglades is a karst system, marine influences naturally extend much further inland than in a non-karst system as the limestone bedrock has a high porosity allowing brackish groundwater discharge (Price et al. 2006). Brackish groundwater discharge naturally increases during the dry season when rainfall and freshwater flow to the coast decreases (Price et al. 2006; Saha et al. 2012). The process of salinization has been exacerbated by reductions in freshwater flow and has led to landscape-scale transitions and loss of vegetative communities (Ross et al. 2000; Saha et al. 2011; Meeder et al. 2017; Andres et al. 2019).

Experimental research in non-tidal, brackish peat marshes of the coastal Everglades suggests the occurrence of open water is driven by declines in above- and belowground biomass and dieback of the dominant emergent

macrophyte, sawgrass (*Cladium jamaincense*), and subsequent peat collapse (Wilson et al. 2018a, b; Andres et al. 2019; Charles et al. 2019). Peat collapse is a "specific type of shallow subsidence unique to highly organic soils in which a loss of soil strength and structural integrity contributes to a decline in elevation, over the course of a few months, to a few years, below the lower limit for emergent plant growth and natural recovery" (Chambers et al. 2019). Non-tidal, brackish marshes generally have deep, highly organic (> 85%) peat soils that rely on biotic inputs from autochthonous production to build soil elevation as they lack mineral inputs via surface water advection. A lack of inorganic mineral inputs makes these marshes highly vulnerable to peat collapse by processes that reduce biologic productivity (Chambers et al. 2019; Ishtiaq et al. 2022).

Understanding what magnitude of elevation loss constitutes collapse requires long-term and precise measurements of elevation change before collapse is initiated. In coastal wetlands this is commonly done using the rod surface elevation table-marker horizon (rSET-MH) approach (Cahoon et al. 2002; Webb et al. 2013; Lynch et al. 2015). The rSET-MH approach has been employed since the late 1990s, with sites existing across the globe (Whelan et al. 2005; Rogers et al. 2006; Wang et al. 2016; Osland et al. 2017; Jankowski et al. 2017; Feher et al. 2022; many others). Some of the benefits of the rSET-MH approach are the repeatability and reliability of measurements over time, and the ability to partition sources of elevation change between surface and subsurface processes (Lynch et al. 2015). Different vegetative communities may contribute more directly to subsurface elevation gain through belowground root production that increases total soil volume and structural integrity (Jafari et al. 2019; Cadigan et al. 2022), or more directly to surface elevation gains through deposition of organic material that vertically accretes over time (Cahoon et al. 2006).

The aim of this study is to inform State and Federal water resource managers about the potential for transitions from vegetated to open water states in brackish, non-tidal peat marshes of the Florida Everglades, by characterizing and relating hydrologic and geomorphic variables across space and time, for different vegetated and unvegetated communities which we refer to as "ecosystem states." We specifically had two objectives. (1) First, we characterize hydrogeomorphic and biologic variability across space via a field survey of hydrogeomorphic conditions and aboveground biomass across emergent (EMG), submerged (SUB), and unvegetated open-water (OW) ecosystem states. (2) Second, we characterize hydrogeomorphic variability over time, specifically in vegetated states (EMG and SUB). We monitored geomorphic changes (soil elevation, vertical accretion) in the SUB state using the rSET-MH approach from June 2018 to May 2023, and monitored bi-monthly porewater salinity changes in the EMG state from November 2019 to July 2022. We monitored the number of dry days where the

soil surface was exposed (water depth ≤ 0 cm) for both SUB and EMG states to evaluate water surface dry-down as a driver of geomorphic and hydrologic change.

For objective 1, we predicted that linear relationships would be found across biologic, hydrologic, and geomorphic variables. Specifically, as values of geomorphic variables (soil surface elevation, soil depth) decrease, hydrologic variables (porewater salinity, water depth) will increase, and the value of our biologic variable (sawgrass biomass) will decrease. Additionally, we predicted: (a) large, relative differences and non-overlapping hydrogeomorphic conditions between EMG and OW states and (b) that differences would be of similar magnitude as studies describing alternate stable states in tidal marshes (Schepers et al. 2020; Wang et al. 2021). For objective 2, we predicted that vertical accretion would be greater than the rate of soil elevation change in the SUB state, with both variables being positively related with the cumulative number of dry days. Additionally, we predicted that porewater salinity in the EMG state would experience seasonal salinization with a relatively large increase in the dry season and that the degree of salinization would be positively related to the number of bi-monthly dry days that occurred between each porewater salinity measurement.

Methods

Study Area

The Florida Everglades is a broad, low-relief landscape located in south Florida, USA, and is the largest wetland in North America. The southernmost region is home to Everglades National Park, a phosphorus-limited, karstic system with a functional "upside-down estuary" where nutrients are primarily derived from marine sources (Childers et al. 2019). Everglades National Park contains an estimated 448,200 ha of diverse wetland, upland, and marine ecosystems, with marsh ecosystems accounting for 48.3% of the landscape (Ruiz et al. 2021). Across marsh vegetation types, *Cladium jamaicense* either dominates or co-dominates 111,487 ha or 24.9% of the landscape (Ruiz et al. 2021). Across the south Florida region rainfall is the primary freshwater input with annual variation split into two seasons: a wet season from May to October and a dry season from November to April (Abiy et al. 2019).

This study took place across 9 ha of non-tidal, brackish peat marsh in the FCE (Fig. 1a and 25°13′13.17″ N, 80°50′36.96″ W). The study site is ~ 7 km northwest of the north shore of Florida Bay (Fig. 1a) but does not exhibit tidal fluctuations (Fig. 1b). Water level fluctuations from Nov 2018 to May 2022 at the study site show similar seasonal variability yet lack the relatively large tidal fluctuations exhibited at Alligator Creek (USGS 2016a), and microtidal fluctuations at West Lake (USGS 2016b) (Fig. 1b). Similar non-tidal brackish marshes can be largely found interspersed around the shallow estuarine bay of Whitewater Bay and near the mangrove lakes along the north shore of Florida Bay, an area that is known to have experienced extensive saltwater intrusion and ecological change during the twentieth century (Tabb et al. 1962; Stewart et al. 2002; Langevin et al. 2005). The site is specifically situated along the northwest side of Main Park Road within Everglades National Park and is connected to a larger wetland area that encompasses ~ 3000 ha between Main Park Road, Coot Bay, Whitewater Bay, and Hell's Bay (Fig. 1a). The study site is dominated by the emergent macrophyte, *Cladium jamaicense* (sawgrass), interspersed by mats of submerged aquatic vegetation that is dominated by the macroalgae *Chara* sp., and unvegetated open water. To a lesser extent, scrub (heights < 1.5 m) *Conocarpus erectus* (buttonwood) and *Rhizophora mangle* scrub (red mangrove) can be found. Soils are histosols (peat) with > 85% organic matter ranging 1.0–2.0 m in depth. In March 2021, a prescribed burn was conducted with high burn severity across the entire study area.

Characterizing Hydrogeomorphic and Biologic Variability Across Space

We conducted a field survey to characterize hydrogeomorphic variability across the study site, initiated in November 2019 and completed in January 2020 (Fig. 2a). The survey was conducted along three 300-m transects, spaced 100 m apart, with survey points positioned roughly every 30 m and stratified across the EMG state (Fig. 2b), SUB state (Fig. 2c), and OW state (Fig. 2d). Percent cover of > 75% of *C. jamaicense* within a 1-m² plot was used to identify the EMG state. Presence of *Chara* sp. and absence of *C. jamaicense* were used to identify the SUB state. The OW state was identified based on the absence of any vegetation. Measurements at each survey point included geomorphic measurements of soil surface elevation and soil depth, and hydrologic measurements of porewater salinity and surface water depth.

Prior to conducting the hydrogeomorphic field survey, static occupations of rSET installations at the study site were done in June 2018 to establish high-precision, elevation benchmarks. Benchmarks were referenced to the 1988 North American Vertical Datum (NAVD88; Geoid 18b) using Trimble R8 global navigation satellite system receiver equipment (Trimble Inc., Sunnyvale, CA, USA). Two static occupations between 4 and 6 h with differences in elevation solutions between the two occupations < 2 cm. Static surveys of ≥ 4 h have been shown to produce horizontal and vertical errors of less than 3 cm at 95% confidence (Gillins et al. 2019). Soil surface elevation was measured using real-time kinematic survey methods using the same Trimble R8 receivers.

Fig. 1 **a** Map showing location of the study site and the nearest coastal monitoring stations in Florida Bay at Alligator Creek and West Lake. The star on the inset shows location of study site within the boundaries of Everglades National Park in south Florida (black line). **b** Hydrographs of water levels (meters) relative to the North American Vertical Datum of 1988 (NAVD88) from June 2018 to May 2022 showing varying tidal influence where the largest tidal fluctuations occur in Alligator Creek (gray), followed by micro-tidal fluctuations at West Lake (blue), and a lack of tidal influence at the study site (black). Horizontal black line is ground surface elevation of the permanent well at the study site (−0.15 m NAVD88).
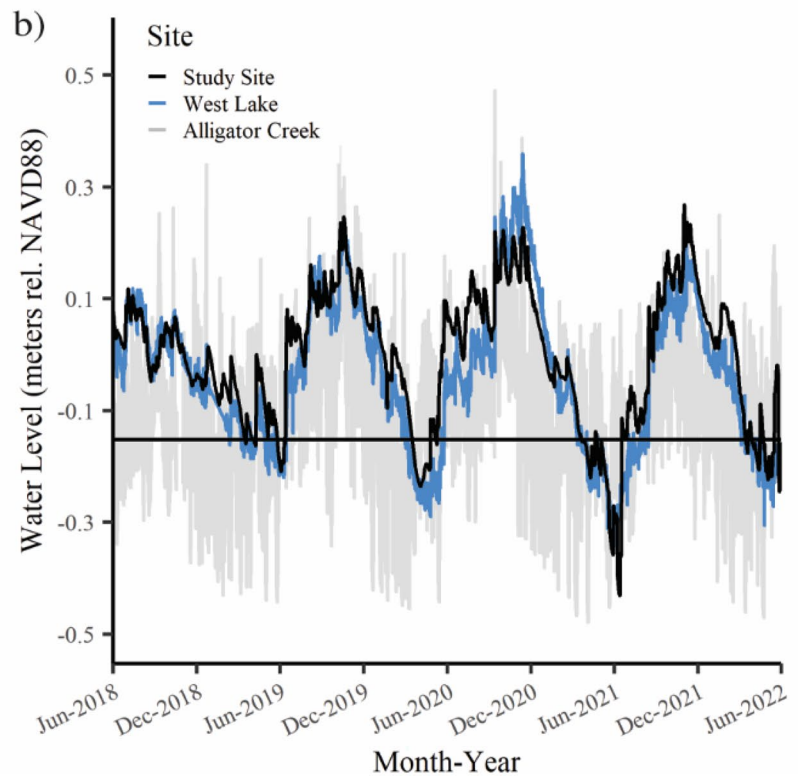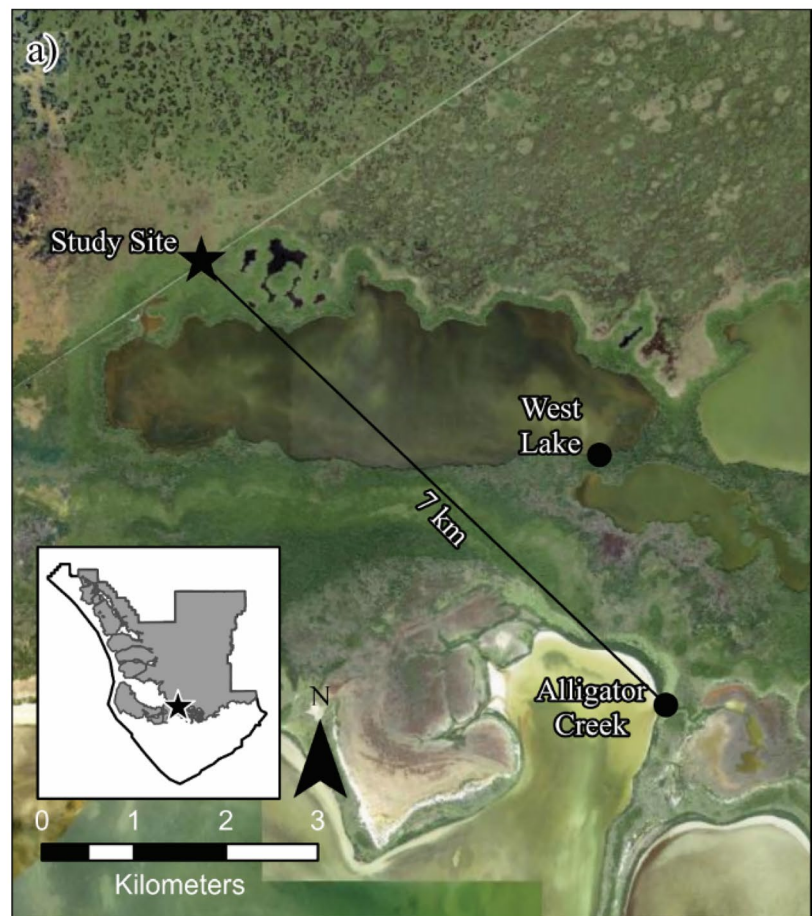
Fig. 2 Site map and ecosystem states surveyed. **a** Location of points surveyed across ecosystem states. Points are color coded by the ecosystem states shown in panels: **b** emergent state (EMG; brown) dominated by *Cladium jamaicense* (sawgrass; brown), **c** submerged state (SUB; red) dominated by *Chara* sp., and **d** unvegetated open-water state (OW; blue). Star indicates location of rod-surface elevation table and marker horizon plots (SET-MH) and permanent well. Crosses indicate location of salinity plots ($n = 9$) where bi-monthly porewater salinity measurements were taken. Inset shows location of the study site (star) within Everglades National Park (black line)
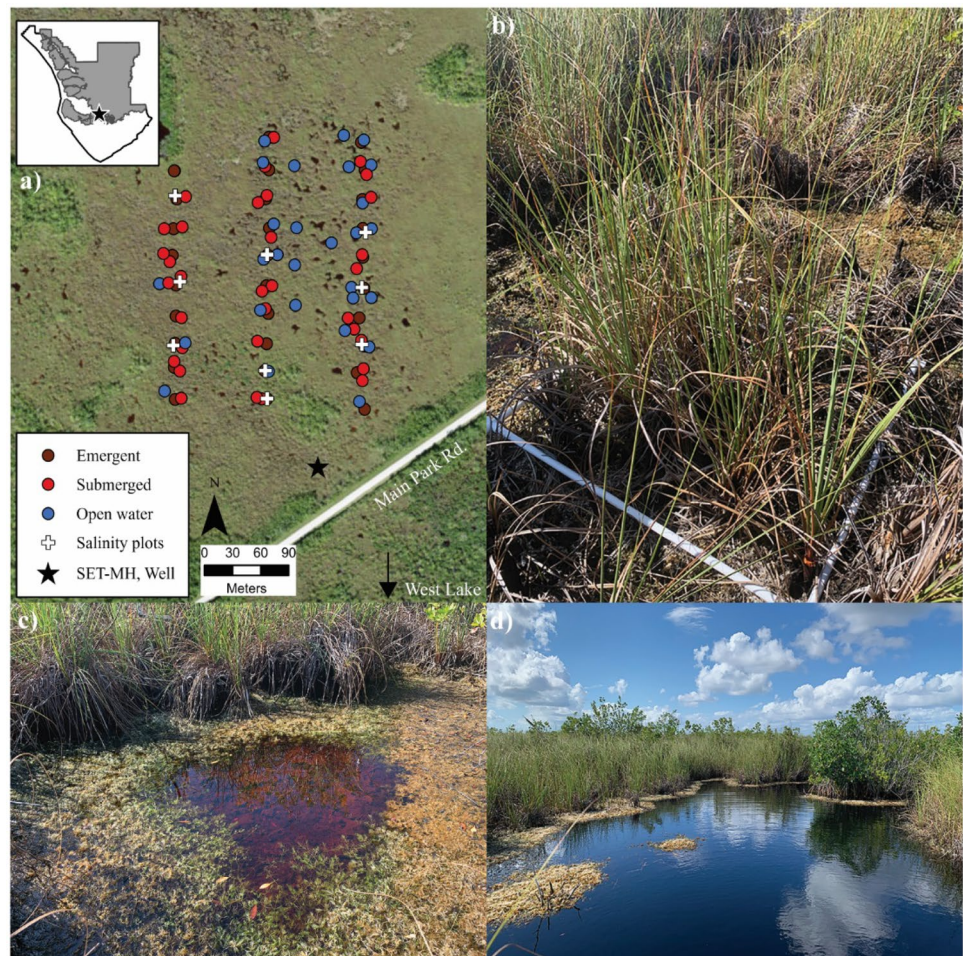
For the hydrogeomorphic survey, soil surface elevation in the EMG and SUB state was measured by gently placing the survey rod on the soil surface. The survey rod was fitted with a topo foot to avoid inserting the survey rod into the soil. Surface water depth was measured simultaneously via centimeter markings on the survey rod. When measuring OW points, there was generally a thick layer of flocculent, unconsolidated sediment, making the soil surface difficult to discern. We standardized measurements by placing the survey rod at the top of the floc layer and allowing it to gently fall through until resistance was met. The point at which resistance was met was identified as the soil surface and subsequent measurements of elevation, soil depth, porewater salinity, and surface water depth were taken. Soil depth was measured at each point using a stainless-steel soil probe by driving the probe through the soil profile to the bedrock. Porewater salinity was measured at a soil depth of 15–30 cm using a YSI Model 600 XL (Xylem, Inc., Yellow Springs, OH, USA). Water depth was measured simultaneously with soil surface elevation, using centimeter markings on the survey rod.

We conducted additional plot-scale measurements of EMG aboveground biomass to characterize aboveground biologic variability across space. At each EMG survey point, we established a 1-m^2 plot to estimate *C. jamaicense* aboveground biomass using a non-destructive phenometric technique developed and validated in the Florida Everglades (Childers et al. 2006). Within 1-m^2 plots, we counted all live individual *C. jamaicense* culms and randomly selected one-third of all individual plants, or a minimum of 15 when the total culm density was less than 45, for further measurement. For this subset, we measured: (1) length of the longest leaf, (2) the culm diameter at the base, and (3) inflorescence height, if present. Biomass for each individual *C. jamaicense* plant measured was estimated using a multiple regression model developed and described in Childers et al. (2006). Total aboveground biomass (g m^{-2}) for each plot was estimated by multiplying culm density per squared meter by mean plant biomass (g dry weight).

Monitoring Hydrogeomorphic Changes in Vegetated States over Time

We evaluated geomorphic changes in the SUB state by monitoring soil elevation change and vertical accretion from June

2018 to May 2023 using the rSET-MH approach (Lynch et al. 2015). Three rSETs were established in May 2017 at the study site within the SUB state following standard methods (Lynch et al. 2015). The rSETs were installed ~ 10 m apart on alternating sides of a permanent, wooden boardwalk at the edge of the study site adjacent to a major road (Fig. 2a). The boardwalk was built prior to rSET installation and provided direct access to the plots from the road without disturbing rSET plots. Following an 11-month equilibration period, baseline soil elevation measurements were made by attaching the rSET instrument to the benchmark, leveling the rSET, and lowering fiberglass pins ($n = 9$) to the soil surface at four fixed azimuths per rSET plot, for $n = 36$ measurements per plot, and 108 measurements total across rSET plots (Fig. 3a). Soil elevation change measurements were made bi-monthly from June 2018 to June 2019, and seasonally from October 2019 to May 2023, except for one additional measurement made in in June 2021.

All rSET plots were in locations that were covered by submerged mats of *Chara* sp. that formed during the wet season (e.g., the SUB state). We removed any *Chara* sp. that was deposited on the soil surface during the dry season so that pin height reflected elevation changes solely from the soil profile. We followed this method for all dry season measurements except in March 2021, when measurements were made shortly after a prescribed fire was conducted that impacted the majority of the study site. Ash deposition and a thick mat of *Chara* sp. made it difficult to remove material without disturbing the soil surface, so pins were lowered on top of the deposited material.

We established five MH plots to monitor vertical accretion at locations characterized by the SUB state along the wooden boardwalk adjacent to rSET plots in May 2017. Marker horizons were established by pouring a white feldspar clay onto the soil surface within a circular bucket with the bottom cut out (circumference = 0.25 m; height of MH layer ~ 5 cm). Feldspar was allowed to settle for 1 month to form an identifiable layer before the bucket was removed. During each soil elevation measurement, MH plots were examined for accreted material. When accretion was observed, a small soil core was extracted and the depth of vertical accretion above the MH was measured in triplicate (Fig. 3b). When the soil surface was dry, a serrated knife was used to cut out a core. When the soil surface was inundated, liquid nitrogen was used to "cryo-core" the MH plot (Lynch et al. 2015).

We evaluated hydrologic changes in the EMG state by monitoring porewater salinity changes in the EMG rooting zone at bi-monthly intervals from November 2019 to July 2022. Measurements were taken across a subset of the EMG aboveground biomass plots established during the field survey, with three plots positioned along each transect, for a total of nine 1-m² plots (Fig. 2a). Six plots were established
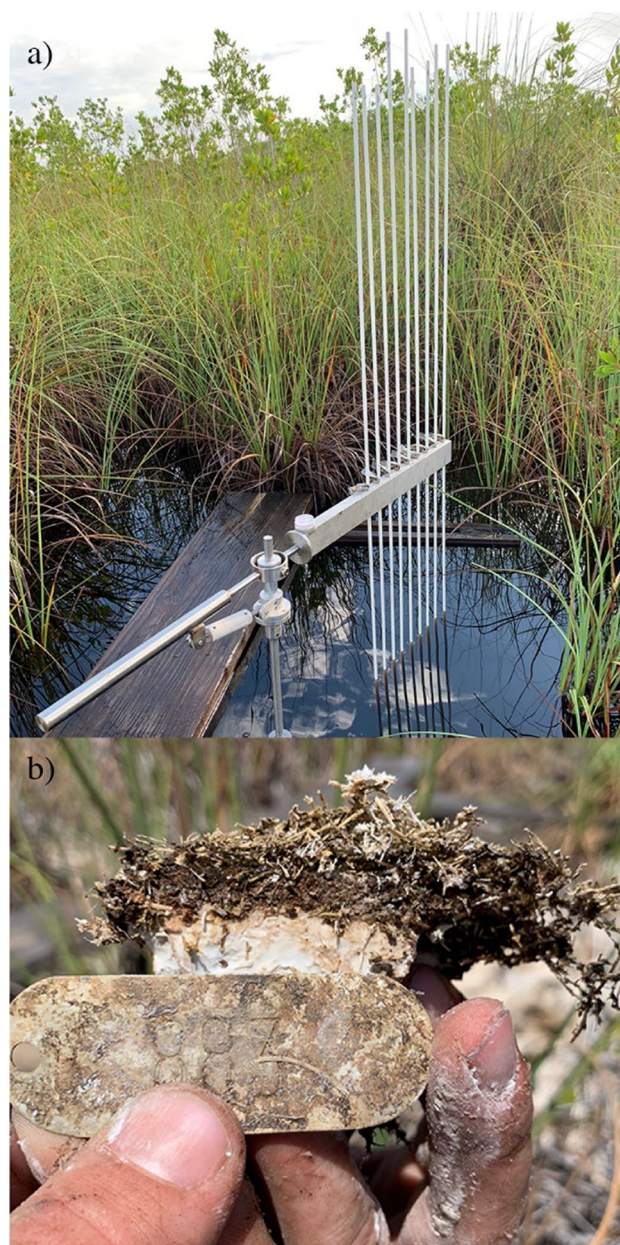

Fig. 3 Overview of rod surface elevation table-marker horizon (SET-MH) measurements. **a** Rod surface elevation table measurements in October 2019. Elevation change is determined based on changes in pin height above the table over time. **b** Marker horizon vertical accretion measurements in March 2021. The white layer is the feldspar marker horizon while the layer above the feldspar layer is vertically accreted material

in November 2019 with additional three plots established in January 2020. Plot locations were selected to cover the range of soil surface elevation and *C. jamaicense* aboveground biomass based on the initial field survey. Porewater salinity measurements were taken in triplicate at fixed points spanning the diagonal axis of each plot with a YSI Model 600 XL probe (Xylem, Inc., Yellow Springs, OH, USA). A porewater

sample was collected at a soil depth of 15–30 cm using a stainless steel "sipper" with a 60-mL syringe attached to a stopcock and rigid tubing. The porewater sample was ejected into a triple-rinsed 100-mL syringe with the probe and measured. Porewater salinity measurements were averaged for each plot and plot averages were averaged together for each bi-monthly sampling period.

We compared geomorphic and hydrologic changes in vegetated states to water surface dry-down by estimating the number of dry days for each state, which is the inverse of hydroperiod and indicates the number of days where the water table drops below the soil surface. We calculated dry days based on the mean ± SD soil surface elevation obtained from the EMG state field survey measurement (Table 1) and mean ± SD of the soil surface elevation for rSET-MH plots (-0.18 ± 0.02 m rel. NAVD88). To estimate dry days, water depth was continuously measured in a permanent well at 30-minute intervals and calibrated monthly for the duration of the study using an AquaTroll 200 (In-Situ Inc., Fort Collins, CO). These data were averaged to the daily scale before calculating the number of dry days. To calculate dry days for EMG plots and rSET-MH plots, we referenced water depth to NAVD88 and subtracted the difference between the soil surface elevation at the well and the mean soil surface elevation of the EMG state (-0.09 ± 0.05 m rel. NAVD88) and rSET-MH plots (-0.18 ± 0.02 m rel. NAVD88). To obtain soil surface elevation at the well, we measured the elevation of top of the well using real-time kinematic surveys (0.61 m rel. NAVD88) and subtracted the height of the well above the soil surface (0.76 m).

Statistical Evaluation

All values are reported as mean ± SD. Prior to analyses, hydrologic and geomorphic variables were checked for outliers that were greater than 1.5 * the interquartile range. This resulted in two SUB and one OW point being removed. We evaluated our first objective by constructing linear mixed effects models to evaluate the strength and direction of relationships between porewater salinity and soil surface elevation, and porewater salinity and soil depth using R package *lme4* (Bates et al. 2015). For both models, we included

ecosystem state as a random intercept term. We used simple linear regression to evaluate relationships between EMG biomass and soil surface elevation, and EMG biomass and porewater salinity using R package *stats* (R Core Team 2023). To estimate the strength of relationships, we calculated overall model R^2, the marginal R^2 (R^2_{marg}) for mixed effects model using R package *MuMIn* (Bartoń 2023), and bootstrap confidence intervals using 1000 model simulations using R package *stats* (R Core Team 2023). Additionally, we evaluated whether EMG and OW states have similar hydrogeomorphic differences as studies from tidal marshes that identify them as alternate stable states (e.g., Schepers et al. 2020), by calculating the degree of overlap between ecosystem states and computed kernel density distributions for elevation, and porewater salinity, using R package *overlapping* (Pastore et al. 2022). Evaluation of frequency distributions has been described as the "spatial analogue" for identifying alternate stable states in space (Scheffer and Carpenter 2003).

We evaluated our second objective by estimating and comparing rates of cumulative soil elevation change and vertical accretion using simple linear regression where cumulative soil elevation change/vertical accretion was regressed against time since the baseline, using R package *stats* (R Core Team 2023). For each rSET plot, prior to calculating cumulative elevation changes, we removed any measurement that had an interval change from the prior measurement of ± 3.6. Across all pin measurements, median ± SD of interval changes was 0 ± 1.8 cm; therefore, 3.6 cm represents removal of pin changes greater than ± 2 SD (Fig. S1). After calculating cumulative elevation change for each pin, cumulative change was averaged for each azimuth, all azimuths averaged for each plot, and all plots averaged together for a single average elevation change value per timepoint. After December 2021, sample size was reduced to $n = 90$ pins as two azimuths were decommissioned due to a board breaking into the plot. For MH plots, the rate of vertical accretion was calculated by averaging vertical accretion measurements for each plot ($n = 5$) at each time point then averaging all plot averages together. We compared rates of geomorphic changes to hydrologic changes by estimating the strength and direction of relationships between soil elevation change and cumulative dry days, and vertical accretion

Table 1 Mean values (± SD) of biologic, hydrologic, and geomorphic variables measured across ecosystem states

Variable	Ecosystem state		
	Emergent (EMG)	Submerged (SUB)	Open water (OW)
Soil elevation (m; NAVD88)	-0.09 ± 0.05	-0.21 ± 0.05	-0.44 ± 0.11
Soil depth (m)	1.56 ± 0.08	1.46 ± 0.07	1.19 ± 0.15
Porewater salinity (ppt)	7.2 ± 1.4	9.6 ± 1.2	12.2 ± 1.18
Water depth (cm)	16.5 ± 7.2	27.9 ± 7.2	46.5 ± 9.0
Aboveground biomass (g m^{-2})	537 ± 332	NA	NA

and cumulative dry days, using simple linear regression. The number of cumulative dry days was calculated for the duration of rSET-MH measurements. We did not include the March 2021 soil elevation change measurement in regression analysis. Additionally, we evaluated hydrologic changes in the EMG state by characterizing the magnitude of seasonal changes in porewater salinity, and dry days, and estimated the strength and direction of relationships using simple linear regression. For bi-monthly porewater salinity measurements, we calculated the number of dry days between each bi-monthly interval from November 2019 to July 2022.

Results

Characterizing Hydrogeomorphic and Biologic Variability Across Space

We surveyed 91 points across EMG ($n = 30$), SUB ($n = 33$), and OW ($n = 28$). A power analysis conducted using R package *pwr* (Champely 2020) indicated that we could estimate a moderate effect with this sample size ($f = 0.33$; $k = 3$; $n = 30$, $\alpha = 0.05$; $\beta = 0.8$). Mean soil surface elevation and soil depth were highest for EMG, followed by SUB and OW (Table 1). Mean porewater salinity and water depth were lowest for EMG, followed by SUB and OW (Table 1). Within EMG plots, *C. jamaicense* aboveground biomass ranged from 138.8 to 1371.4 g m^{-2}, with a mean value of 537.2 ± 332.1 g m^{-2} (Table 1).

Across hydrologic, geomorphic, and biologic variables, linear trends were observed (Fig. 4). Porewater salinity decreased linearly as soil surface elevation increased (Fig. 4a; $R^2_{marg} = 0.75$, $R^2 = 0.81$, slope $= -12.4$, 95% CI [-15.1 to -9.7], $n = 88$), and as soil depth increased (Fig. 4b; $R^2_{marg} = 0.16$, $R^2 = 0.71$, slope $= -4.9$, 95% CI [-7.3 to -2.5], $n = 88$). Emergent aboveground biomass increased linearly with soil surface elevation with a large effect size (Fig. 4c; $R^2 = 0.19$, slope $= 26.9$, 95% CI [7.3 to 46.2], $n = 29$), and decreased linearly as porewater salinity increased with a large effect size (Fig. 4d; $R^2 = 0.17$, slope $= -109.7$, 95% CI [-194.0 to -25.3], $n = 29$).

Kernel density distributions show little to no overlap in the hydrogeomorphic conditions of the EMG and OW states. Frequency distributions of elevation and porewater

Fig. 4 Linear regression analyses that show strength and direction of relationships across ecosystem states between: **a** soil surface elevation (m; rel. to the North American Vertical Datum of 1988) and porewater salinity (ppt), **b** soil depth (m) and porewater salinity, **c** emergent aboveground biomass (g m^{-2}) and soil surface elevation, and **d** emergent biomass and porewater salinity. Color indicates ecosystem state: emergent marsh (EMG; brown), submerged marsh (SUB; red), and unvegetated open water (OW; blue)
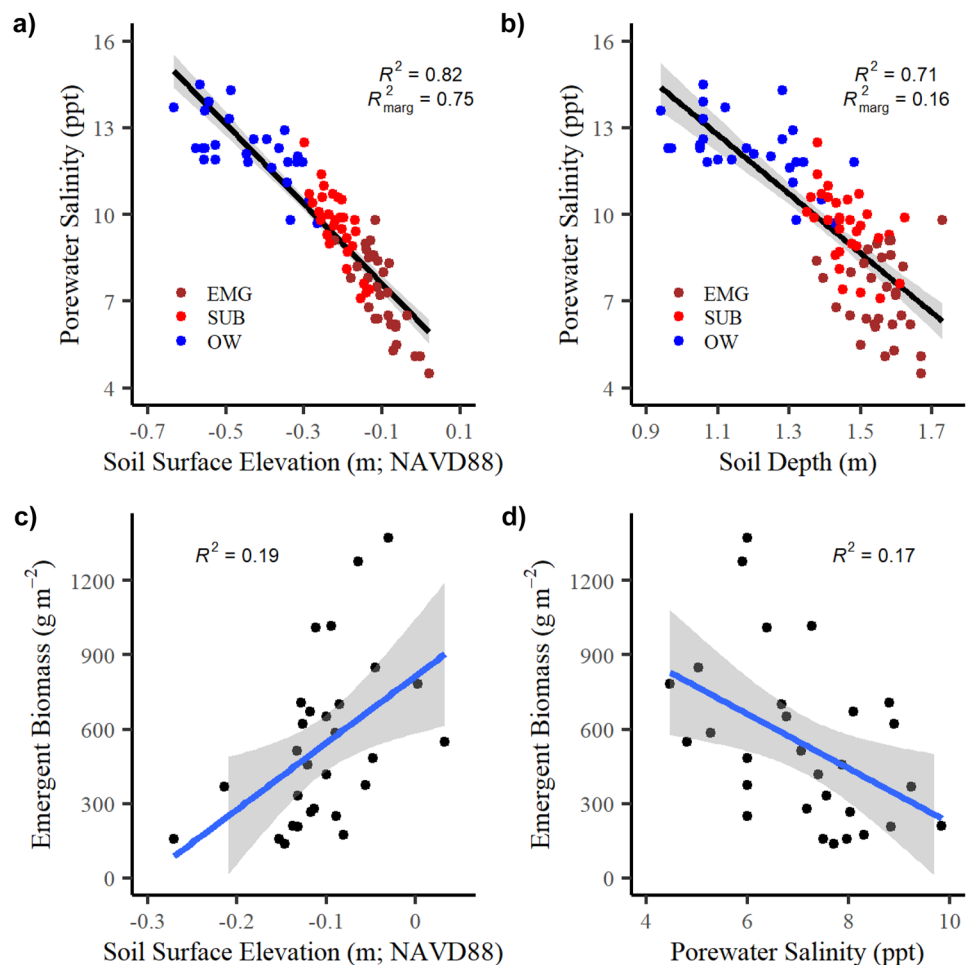
salinity exhibited an area of overlap of 3% and 6%, respectively (Fig. 5). A relatively greater percent area overlap was found between EMG and SUB states, with 18% and 27%, for elevation and porewater salinity, respectively (Fig. 5). Intermediate percent area overlap was found between SUB and OW, with 12% and 15%, for elevation and porewater salinity, respectively (Fig. 5).

Monitoring Hydrogeomorphic Changes in Vegetated States over Time

In the SUB state from June 2018 to May 2023, we estimated a -1.14 ± 0.74 mm year^{-1} rate of cumulative soil surface elevation change (Fig. 6a), and a 2.3 ± 0.95 mm year^{-1} rate of vertical accretion (Fig. 6b). No vertical accretion was observed until March 2020 and standard error increased over time (Fig. 6b). Mean rSET station soil surface elevation relative to NAVD88 was -0.18 ± 0.02 m, which is in range with the SUB state soil surface elevation measured across field survey points (Table 1). Variability in soil elevation changes was observed across plots, with two plots declining in elevation and one station showing a slight increase in elevation (Fig. S2). Soil elevation change decreased linearly as cumulative dry days increased (Fig. 6c; $R^2 = 0.33$, slope $= -0.04$, 95% CI [-0.07 to -0.009], $n = 15$). Vertical accretion generally increased as cumulative dry days increased;

Fig. 5 Kernel density distributions for **a** porewater salinity (ppt) and **b** soil surface elevation (m; rel. to the North American Vertical Datum of 1988), across ecosystem states: emergent marsh (EMG; brown), submerged marsh (SUB; red), and unvegetated open water (OW; blue). Dashed line indicates mean value for each ecosystem state

however, the strength of this relationship was relatively low (Fig. 6d; $R^2 = 0.13$, slope $= 0.05$, 95% CI [-0.02 to 0.12], $n = 10$).

In the EMG state from November 2019 to July 2022, rooting zone porewater salinity varied seasonally, with relatively large increases between January and July (Fig. 7a). Specifically, between January 2021 and July 2021, porewater salinity increased from 8.8 ± 0.6 to 16.5 ± 2.1 ppt (Fig. 7). Similarly, between January and May 2022, porewater salinity increased from 9.9 ± 1.6 to 16.2 ± 1.3 ppt (Fig. 7). Average dry season salinization for these two seasons was $+7.0$ ppt. Only a slight increase in porewater salinity was observed in 2020. Dry days occurred between March and July, contingent on rainfall patterns (Fig. 7b). While dry days occurred between March and May 2020, only a small increase in porewater salinity was observed. When comparing total rainfall based on a nearby United States Geologic Survey monitoring station ~6 km from the study site (station name = "NMP"), this bi-monthly interval saw increased rainfall relative to the same interval in 2021 and 2022, which may have mitigated seasonal salinization (Fig. 7b). Porewater salinity increased linearly as the number of dry days increased (Fig. 7c; $R^2 = 0.45$, slope $= 0.09$, 95% CI [0.04 to 0.14], $n = 16$).

Discussion

The characterization of hydrogeomorphic conditions in coastal marshes, both across space and time, can provide insight into local variability and inform land managers about the potential for transitions between alternate stable states that would signal marsh loss. Our objectives helped to differentiate and describe processes that are indicative of alternative stable states as they are described in the literature for tidal marsh systems (Schepers et al. 2020; Wang et al. 2021). Our study contributes to this body of knowledge regarding transitions between vegetated and open water alternate states by expanding into a non-tidal peat marsh experiencing salinization.

Consistent with our predictions for objective 1, we found that across vegetated and unvegetated marsh ecosystem states, hydrogeomorphic conditions were negatively related (Fig. 4a and b). Further, EMG aboveground biomass was positively related to soil surface elevation and negatively related to porewater salinity (Fig. 4b and c). Between the EMG and OW states, we observed a mean difference in soil surface elevation of 35 cm, with the OW state found consistently at the lowest soil surface elevations (Table 1). This magnitude of difference is consistent with studies conducted in tidal marshes that describe EMG and OW as alternate states (Stagg et al. 2021; Schepers et al. 2020; Wang et al. 2021). Density distributions further indicated little-to-no
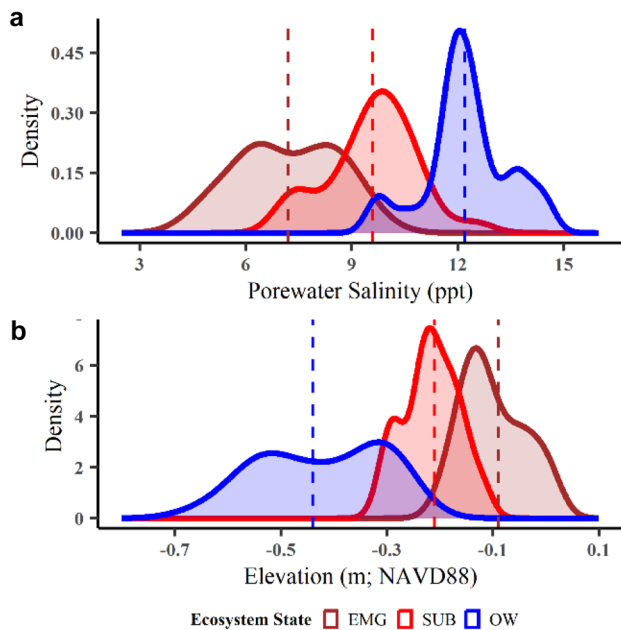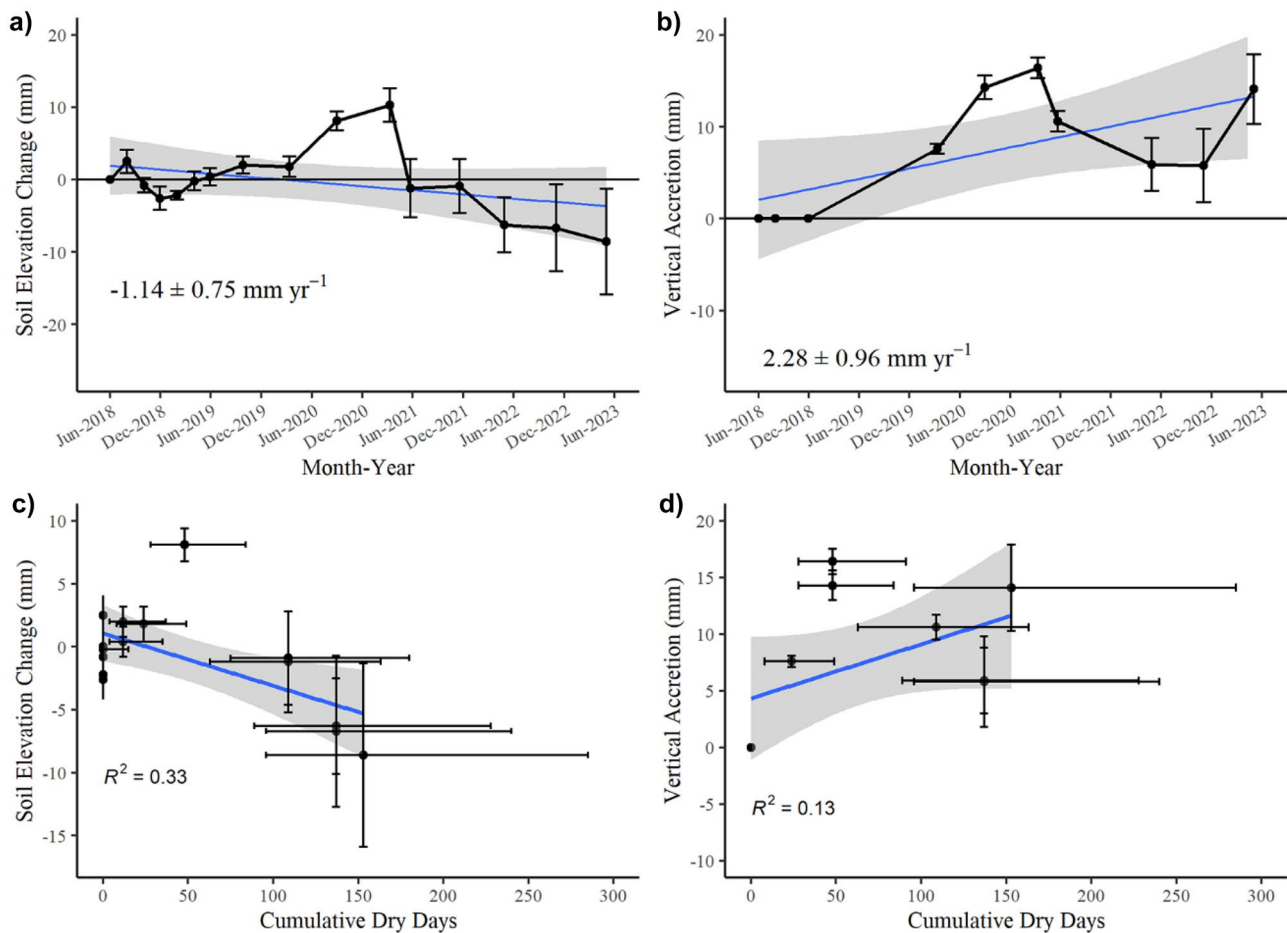
Fig. 6 a Cumulative soil elevation change and **b** vertical accretion from June 2018 to May 2023, in a location characterized as the submerged (SUB) ecosystem state. Note that soil elevation measurements in September 2020 and March 2021 include soil elevation plus vertically accreted material. All other elevation change measurements had vertically accreted material removed from soil surface prior to measurement. Values are mean ± SE. **c** Cumulative soil elevation change and **d** vertical accretion regressed against cumulative dry days (days). Note different scales of y-axes. Horizontal error bars are cumulative dry days ± 2 cm, or the standard deviation of rSET-MH plot soil surface elevation

overlap in the hydrogeomorphic conditions where EMG and OW states were found (Fig. 5). Collectively, these results show that EMG and OW ecosystem states can be differentiated by distinct hydrogeomorphic conditions, while the SUB state can be found at hydrogeomorphic conditions that can overlap EMG and OW states.

Consistent with our predictions for objective 2, we found that the rate of vertical accretion was greater than the rate of soil elevation change in the SUB state, although vertical accretion showed increased variability in the last year of measurement (Fig. 6b). Increased variability of vertical accretion measurements is likely indicative of increased heterogeneity in the floating mats of submerged vegetation dominated by *Chara* sp. as it has been shown to be highly sensitive to salinity and will shift to a microalgal dominated state as salinity and nutrient availability increase (Frankovich et al. 2011, 2012). As dry days cumulatively increased

over the 5-year period of rSET-MH measurements, soil elevation declined while vertical accretion increased; however, vertical accretion showed a weaker relationship with cumulative dry days than soil elevation change (Fig. 6c and d). This result could be indicative of a dry day-accretion threshold where water surface dry-down promotes the deposition of submerged vegetation, yet this material can still be oxidized if dry days are prolonged, or the material is "floated" off the soil surface once the water table rises above the soil surface.

The higher rate of vertical accretion relative to soil elevation change was consistent with our prediction and is intuitive given the rSET-MH plots are largely devoid of *C. jamaicense*, which would be needed for belowground soil expansion through root production (Cahoon et al. 2006). The decline in soil surface elevation that occurred during the fourth and fifth years of measurement is most likely

Fig. 7 **a** Porewater salinity (ppt) of the emergent (EMG) state in the rooting zone (soil depth = 15–30 cm) from Nov 2019 to May 2022, averaged across plots (*n* = 9) within the study site. Values are mean ± SD. **b** The number of bi-monthly dry days (black line) for the EMG state and total bi-monthly rainfall (mm; blue line) from a nearby water monitoring station (station name = NMP) from Nov 2019 to May 2022. Error bars are dry days calculated ± 5 cm, or the standard error of EMG soil surface elevation. **c** Relationship between porewater salinity and dry days for each bi-monthly measurement interval
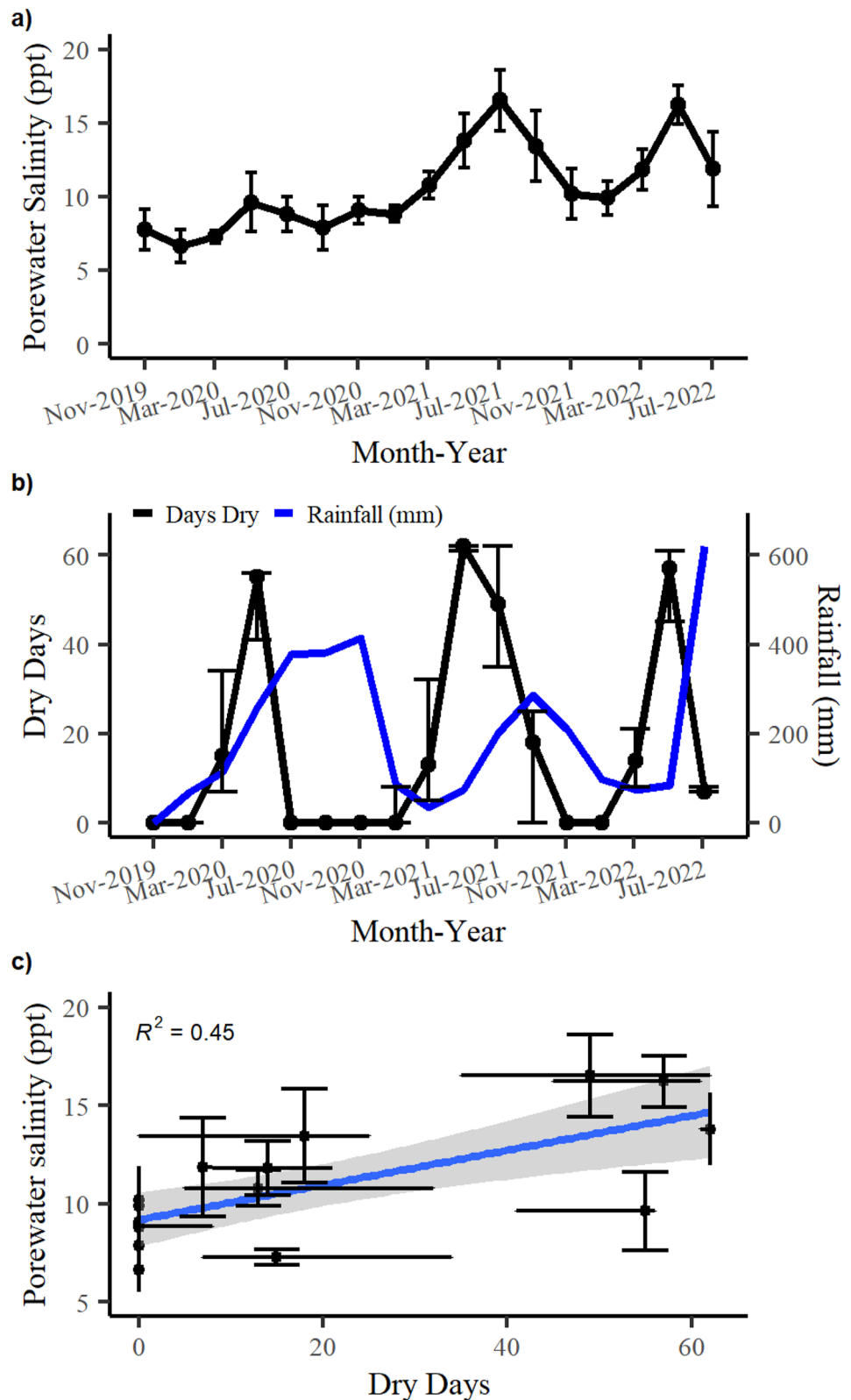
the result of gravity-driven pore space compression that occurred during periods of soil exposure. However, it was not of the magnitude of estimates of peat collapse across the literature, which generally range from 1 to 15 cm and occurs over 5 months to 3 years (Chambers et al. 2019). Given that the period of rSET-MH measurements is relatively short when compared to other rSET-MH sites in the Everglades that have been measured for over 20 years (Feher et al. 2022), it is possible that we captured only the initial stage of collapse and merely one extreme dry season will cause a collapse event that drives a high magnitude loss of soil elevation. Indeed, droughts periodically occur in south Florida and rainfall trends over the last century suggest that the wet season is becoming more unimodal as more rainfall is occurring in the summer months, effectively lengthening dry season conditions, or periods of little to no rainfall (Abiy et al. 2019).

Based on the hydrogeomorphic relationships observed across ecosystem states from objective 1 (Figs. 4 and 5), the long-term changes and relationships of hydrogeomorphic conditions from objective 2 (Figs. 6 and 7), and considering the results of experimental manipulations at the study site

and in outdoor mesocosms indicating salt stress to *C. jamaicense* (Wilson et al. 2018a, b; Charles et al. 2019; Ishtiaq et al. 2022), we propose a conceptual model to explain the driver-response relationships in coastal Everglades non-tidal brackish peat marshes (Fig. 8). Over time, abrupt but temporary seasonal dry-down of the water surface below the soil surface can drive loss of soil elevation in the SUB state, through the physical processes of compaction and oxidation (Fig. 6; Chambers et al. 2019). As a result of dry season soil exposure, salinization of porewater in the surface soils can occur (Fig. 7), reaching salinity levels that increase *C. jamaicense* stress and productivity decline (Troxler et al. 2014; Wilson et al. 2018a, b; Charles et al. 2019; Ishtiaq et al. 2022). If salt stress leads to decreased production and mortality of live tissues, particularly belowground, additional soil elevation loss can occur through the compaction of aerenchyma cells within root tissue (Charles et al. 2019; Chambers et al. 2019), which will exacerbate the ongoing soil elevation loss via physical processes. As elevation is lost in the EMG state, hydrogeomorphic conditions will shift to lower elevations and deeper water depths, allowing *Chara* sp. to colonize
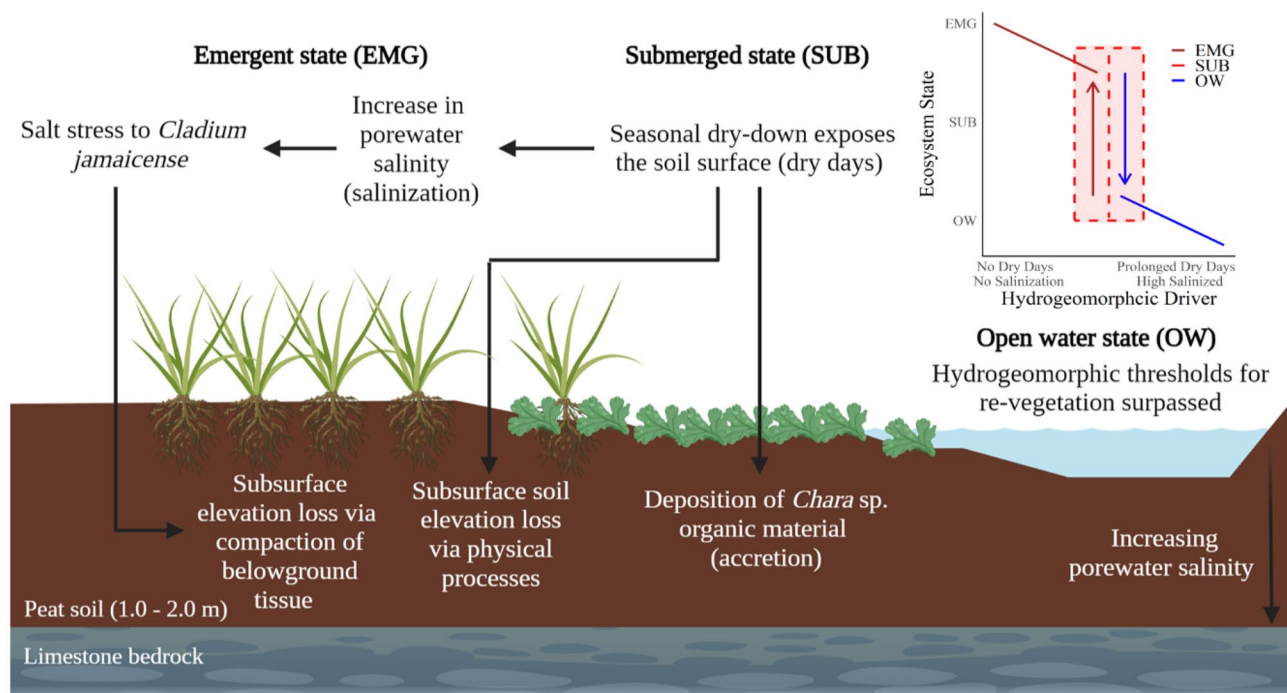

Fig. 8 Diagram depicting ecosystem states and how prolonged seasonal dry-down that exposes the soil surface (dry day) can cause salinization of porewater salinity and affect emergent vegetation and drive soil surface elevation change in non-tidal, brackish peat marshes. Mechanisms describing salt stress to *Cladium jamaicense* and subsurface elevation loss are supported by Ishtiaq et al. (2022); Wilson et al. (2018a, b); and Charles et al. (2019). All other mechanisms are supported by data within this study. Inset is a conceptual example of the threshold state shift that can occur between the alternate emergent (EMG) marsh state and open water (OW) state. Colors indicate ecosystem states. Dashed red lines indicate the range of overlapping hydrogeomorphic conditions that the submerged (SUB) state persists across. Threshold shifts may be contingent on the SUB state, which can mitigate elevation loss through vertical accretion of submerged organic material and slow or prevent hysteretic transitions (upward brown arrow). If the magnitude or duration of salinization or dry days is too large, the SUB state may decline and increase threshold shifts to the OW state (downward blue arrow)

and stabilize surface elevation decline via the deposition of organic material (Fig. 6b). However, when prolonged dry-down also causes salinization, mats of *Chara* sp. may become more heterogeneous and decline due to its low salt tolerance (Frankovich et al. 2012). As *Chara* sp. declines, further salt stress and ultimately mortality of *C. jamaicense* can cause a threshold state shift between the alternate EMG and OW states. Since elevation loss decreases the proximity of the soil surface to the karstic aquifer and brackish groundwater, as elevation is lost, water depth and porewater salinity will increase (Fig. 4). This positive feedback suggests hydrologic thresholds for revegetation by *C. jamaicense* will be surpassed (Pulido et al. 2020) and lead to the persistence of the alternate OW state (Fig. 8).

Current sea-level rise rates for the coastal Everglades are estimated at around 6 mm year^{-1} (Parkinson and Wdowinski 2022), indicating the saltwater front will continue to intrude landward and increase the spatial extent of non-tidal brackish water conditions. There is considerable uncertainty with respect to precipitation trends in the future, although a shift toward a more unimodal rainfall regime (increased summer rainfall) and increasing dry season duration has already been observed over the last century (Abiy et al. 2019). When seasonal salinization is considered with respect to the rate of sea-level rise and potential increase in dry season duration, the abrupt but temporary seasonal salinization reported here may become more persistent and increase in magnitude, which may increase threshold shifts from EMG to OW ecosystem states (Fig. 8 inset; *sensu* Ratajczak et al. 2018). This underscores the importance of continued progress on Everglades restoration projects that aim to increase the volume of freshwater being delivered to coastal wetlands, as it is the primary management intervention available to mitigate the salinization of freshwater and brackish peat marshes. The expansion of hydrogeomorphic monitoring sites within non-tidal and tidal brackish peat marshes, both for field surveys and to establish permanent wells and SET-MH plots, would greatly increase our ability to monitor changing hydrogeomorphic conditions, both across vegetated states and the landscape, and help inform water managers and guide further research into understanding the potential areal extent and trajectories of ecosystem state changes across the coastal Everglades.

References

Abiy, A.Z., A.M. Melesse, W. Abtew, and D. Whitman. 2019. Rainfall trend and variability in Southeast Florida: implications for freshwater availability in the Everglades. *PloS One* 14: e0212008.

Andres, K., M. Savarese, B. Bovard, and M. Parsons. 2019. Coastal wetland geomorphic and vegetative change: effects of sea-level rise and water management on brackish marshes. *Estuaries and Coasts* 42: 1308–1327.

Bartoń, K. 2023. *MuMIn: Multi-model Inference*. R package version 1.47.5. https://CRAN.R-project.org/package=MuMIn.

Bates, D., M. Mächler, B. Bolker, and S. Walker. 2015. Fitting linear mixed-effects models using lme4. *Journal of Statistical Software* 67: 1–48.

Beisner, B.E., D.T. Haydon, and K. Cuddington. 2003. Alternative stable states in ecology. *Frontiers in Ecology and the Environment* 1: 376–382.

Cadigan, J.A., N.H. Jafari, C.L. Stagg, C. Laurenzano, B.D. Harris, A.E. Meselhe, J. Dugas, and B. Couvillion. 2022. Characterization of vegetated and ponded wetlands with implications towards coastal wetland marsh collapse. *Catena* 218: 106547.

Cahoon, D.R., J.C. Lynch, B.C. Perez, B. Segura, R.D. Holland, C. Stelly, G. Stephenson, and P. Hensel. 2002. High-precision measurements of wetland sediment elevation: II. The rod surface elevation table. *Journal of Sedimentary Research* 72: 734–739.

Cahoon, D.R., P.F. Hensel, T. Spencer, D.J. Reed, K.L. McKee, and N. Saintilan. 2006. Coastal wetland vulnerability to relative sea-level rise: wetland elevation trends and process controls. In *Wetlands and natural resource management*, ed. J.T.A. Verhoeven, B. Beltman, R. Bobbink, and D. Whigham, 271–292. Berlin: Springer.

Chambers, L.G., H.E. Steinmuller, and J.L. Breithaupt. 2019. Toward a mechanistic understanding of peat collapse and its potential contribution to coastal wetland loss. *Ecology* 100: e02720.

Champely, S. 2020. *pwr: Basic functions for power analysis.* R package version 1.3-0. https://CRAN.R-project.org/package=pwr.

Charles, S.P., J.S. Kominoski, T.G. Troxler, E.E. Gaiser, S. Servais, B.J. Wilson, S.E. Davis, F.H. Sklar, C. Coronado-Molina, and C.J. Madden. 2019. Experimental saltwater intrusion drives rapid soil elevation and carbon loss in freshwater and brackish Everglades marshes. *Estuaries and Coasts* 42: 1868–1881.

Childers, D.L., D. Iwaniec, D. Rondeau, G. Rubio, E. Verdon, and C.J. Madden. 2006. Responses of sawgrass and spikerush to variation in hydrologic drivers and salinity in Southern Everglades marshes. *Hydrobiologia* 569: 273–292.

Childers, D.L., E. Gaiser, and L.A. Ogden. 2019. *The Coastal everglades: the dynamics of social-ecological transformation in the South Florida landscape.* New York: Oxford University Press, USA.

R Core Team. 2023. R: a language and environment for statistical computing. R Foundation for Statistical Computing, Vienna, Austria. https://www.R-project.org/.

Dessu, S.B., R.M. Price, T.G. Troxler, and J.S. Kominoski. 2018. Effects of sea-level rise and freshwater management on long-term water levels and water quality in the Florida Coastal Everglades. *Journal of Environmental Management* 211: 164–176.

Enwright, N.M., K.T. Griffith, and M.J. Osland. 2016. Barriers to and opportunities for landward migration of coastal wetlands with sea-level rise. *Frontiers in Ecology and the Environment* 14: 307–316.

Fagherazzi, S., L. Carniello, L. D'Alpaos, and A. Defina. 2006. Critical bifurcation of shallow microtidal landforms in tidal flats and salt marshes. Proceedings of the National Academy of Sciences 103: 8337–8341.

Feher, L. C., M. J. Osland, K. L. McKee, K. R. Whelan, C. Coronado-Molina, F. H. Sklar, K. W. Krauss, R. J. Howard, D. R. Cahoon, J. C. Lynch, L. Lamb-Wotton, T. Troxler, J. R. Conrad, G. Anderson, W. C. Vervaeke, T. J. Smith III, N. Cormier, A. S. From, and L. Allain. 2022. Soil elevation change in mangrove forests and marshes of the Greater Everglades: a regional synthesis of surface elevation table-marker horizon (SET-MH) data. Estuaries and Coasts: 1–30.

Frankovich, T.A., D. Morrison, and J.W. Fourqurean. 2011. Benthic macrophyte distribution and abundance in estuarine mangrove lakes and estuaries: relationships to environmental variables. *Estuaries and Coasts* 34: 20–31.

Frankovich, T.A., J.G. Barr, D. Morrison, and J.W. Fourqurean. 2012. Differing temporal patterns of *Chara hornemannii* cover correlate to alternate regimes of phytoplankton and submerged aquatic-vegetation dominance. *Marine and Freshwater Research* 63: 1005–1014.

U.S. Geological Survey (USGS). 2016b. National Water Information System data available on the World Wide Web (USGS Water Data for the Nation). https://waterdata.usgs.gov/monitoring-location/251203080480600/#parameterCode=00065.=P7D. Accessed 02 December 2022.

U.S. Geological Survey (USGS). 2016a. National Water Information System data available on the World Wide Web (USGS Water Data for the Nation). https://waterdata.usgs.gov/monitoring-location/251032080473400/#parameterCode=00065.=P7D. Accessed 02 December 2022.

Gillins, D.T., D. Kerr, and B. Weaver. 2019. Evaluation of the online positioning user service for processing static GPS surveys: OPUS-Projects, OPUS-S, OPUS-Net, and OPUS-RS. *Journal of Surveying Engineering* 145: 1–14.

Herbert, E.R., P. Boon, A.J. Burgin, S.C. Neubauer, R.B. Franklin, M. Ardón, K.N. Hopfensperger, L.P. Lamers, and P. Gell. 2015. A global perspective on wetland salinization: ecological consequences of a growing threat to freshwater wetlands. *Ecosphere* 6: 1–43.

Ishtiaq, K. S., T. G. Troxler, L. Lamb-Wotton, B. J. Wilson, S. P. Charles, S. E. Davis, J. S. Kominoski, D. T. Rudnick, and F. H. Sklar. 2022. Modeling net ecosystem carbon balance and loss in coastal wetlands exposed to sea-level rise and saltwater intrusion. Ecological Applications: e2702.

Jafari, N. H., B. D. Harris, J. A. Cadigan, J. W. Day, C. E. Sasser, G. P. Kemp, C. Wigand, A. Freeman, L. A. Sharp, and J. Pahl. 2019. Wetland shear strength with emphasis on the impact of nutrients, sediments, and sea level rise. Estuarine, Coastal and Shelf Science 229: 106394.

Jankowski, K.L., T.E. Törnqvist, and A.M. Fernandes. 2017. Vulnerability of Louisiana's coastal wetlands to present-day rates of relative sea-level rise. *Nature Communications* 8: 14792.

Langevin, C., E. Swain, and M. Wolfert. 2005. Simulation of integrated surface-water/ground-water flow and salinity for a coastal wetland and adjacent estuary. *Journal of Hydrology* 314: 212–234.

Lynch, J. C., P. Hensel, and D. R. Cahoon. 2015. The surface elevation table and marker horizon technique: a protocol for monitoring wetland elevation dynamics. Natural Resource Report NPS/NCBN/NRR—2015/1078. National Park Service, Fort Collins, Colorado. https://pubs.usgs.gov/publication/70160049.

Marani, M., C. Da Lio, and A. D'Alpaos. 2013. Vegetation engineers marsh morphology through multiple competing stable states. Proceedings of the National Academy of Sciences 110: 3259–3263.

McVoy, C., W.P. Said, J. Obeysekera, J.A. VanArman, and T.W. Dreschel. 2011. *Landscapes and hydrology of the pre-drainage Everglades.* Florida: University Press of Florida Gainesville.

Meeder, J.F., R.W. Parkinson, P.L. Ruiz, and M.S. Ross. 2017. Saltwater encroachment and prediction of future ecosystem response to the Anthropocene Marine Transgression, Southeast saline Everglades, Florida. *Hydrobiologia* 803: 29–48.

Moffett, K.B., W. Nardin, S. Silvestri, C. Wang, and S. Temmerman. 2015. Multiple stable states and catastrophic shifts in coastal wetlands: progress, challenges, and opportunities in validating theory using remote sensing and other methods. *Remote Sensing* 7: 10184–10226.

Osland, M.J., K.T. Griffith, J.C. Larriviere, L.C. Feher, D.R. Cahoon, N.M. Enwright, D.A. Oster, J.M. Tirpak, M.S. Woodrey, and R.C. Collini. 2017. Assessing coastal wetland vulnerability to sea-level rise along the northern Gulf of Mexico coast: gaps and opportunities for developing a coordinated regional sampling network. *PloS One* 12: e0183431.

Osland, M.J., B. Chivoiu, N.M. Enwright, K.M. Thorne, G.R. Guntenspergen, J.B. Grace, L.L. Dale, W. Brooks, N. Herold, and J.W. Day. 2022. Migration and transformation of coastal wetlands in response to rising seas. *Science Advances* 8: eabo5174.

Pastore, M., P. A. D. Loro, M. Mingione, A. Calcagni. 2022. *Overlapping: Estimation of overlapping in empirical distributions.* R package version 2.1. https://CRAN.R-project.org/package=overlapping.

Parkinson, R. W., and S. Wdowinski. 2022. Accelerating sea-level rise and the fate of mangrove plant communities in South Florida, USA. Geomorphology: 108329.

Price, R.M., P.K. Swart, and J.W. Fourqurean. 2006. Coastal groundwater discharge–an additional source of phosphorus for the oligotrophic wetlands of the Everglades. *Hydrobiologia* 569: 23–36.

Pulido, C., N. Sebesta, and J.H. Richards. 2020. Effects of salinity on sawgrass (Cladium jamaicense Crantz) seed germination. *Aquatic Botany* 166: 103277.

Raposa, K.B., A. Woolfolk, C.A. Endris, M.C. Fountain, G. Moore, M. Tyrrell, R. Swerida, S. Lerberg, B.J. Puckett, and M.C. Ferner. 2023. Evaluating thin-layer sediment placement as a tool for enhancing tidal marsh resilience: a coordinated experiment across

eight US National Estuarine Research Reserves. *Estuaries and Coasts* 14: 595–615.

Ratajczak, Z., S.R. Carpenter, A.R. Ives, C.J. Kucharik, T. Ramiadantsoa, M.A. Stegner, J.W. Williams, J. Zhang, and M.G. Turner. 2018. Abrupt change in ecological systems: inference and diagnosis. *Trends in Ecology & Evolution* 33: 513–526.

Rogers, K., K. Wilton, and N. Saintilan. 2006. Vegetation change and surface elevation dynamics in estuarine wetlands of southeast Australia. Estuarine, Coastal and Shelf Science 66: 559–569.

Ross, M., J. Meeder, J. Sah, P. Ruiz, and G. Telesnicki. 2000. The southeast saline Everglades revisited: 50 years of coastal vegetation change. *Journal of Vegetation Science* 11: 101–112.

Ruiz, P.L., T.N. Schall, R.B. Shamblin, and K.R.T. Whelan. 2021. The vegetation of Everglades National Park: final report. In *Natural resource report NPS/SFCN/NRR—2021/2256*. Colorado: National Park Service, Fort Collins. https://doi.org/10.36967/nrr-2286460.

Saha, A.K., S. Saha, J. Sadle, J. Jiang, M.S. Ross, R.M. Price, L.S. Sternberg, and K.S. Wendelberger. 2011. Sea level rise and South Florida coastal forests. *Climatic Change* 107: 81–108.

Saha, A.K., C.S. Moses, R.M. Price, V. Engel, T.J. Smith, and G. Anderson. 2012. A hydrological budget (2002–2008) for a large subtropical wetland ecosystem indicates marine groundwater discharge accompanies diminished freshwater flow. *Estuaries and Coasts* 35: 459–474.

Scheffer, M., and S.R. Carpenter. 2003. Catastrophic regime shifts in ecosystems: linking theory to observation. *Trends in Ecology & Evolution* 18: 648–656.

Schepers, L., P. Brennand, M.L. Kirwan, G.R. Guntenspergen, and S. Temmerman. 2020. Coastal marsh degradation into ponds induces irreversible elevation loss relative to sea level in a microtidal system. *Geophysical Research Letters* 47 e2020GL089121.

Sklar, F.H., J.F. Meeder, T.G. Troxler, T. Dreschel, S.E. Davis, and P.L. Ruiz. 2019. The Everglades: at the forefront of transition. In *Coasts and estuaries*, ed. E. Wolanski, J. Day, M. Elliot, and R. Ramachandran, 277–292. Oxford: Elsevier.

Stagg, C.L., M.J. Osland, J.A. Moon, L.C. Feher, C. Laurenzano, T.C. Lane, W.R. Jones, and S.B. Hartley. 2021. Extreme precipitation and flooding contribute to sudden vegetation dieback in a coastal salt marsh. *Plants* 10: 1841.

Stewart, M., T. Bhatt, R. Fennema, and D. Fitterman. 2002. The road to Flamingo: An evaluation of flow pattern alterations and salinity intrusion in the lower glades, Everglades National Park. *Open-File Report*, 02–59 US Department of the Interior, US Geological Survey, Menlo Park, CA, USA.

Sweet, W. V., B. D. Hamlington, R. E. Kopp, C. P. Weaver, P. L. Barnard, D. Bekaert, W. Brooks, M. Craghan, G. Dusek, T. Frederikse, G. Garner, A. S. Genz, J. P. Krasting, E. Larour, D. Marcy, J. J. Marra, J. Obeysekera, M. Osler, M. Pendleton, D. Roman, L. Schmied, W. Veatch, K. D. White, and C. Zuzak. 2022. Global and Regional Sea Level Rise Scenarios for the United States: Updated Mean Projections and Extreme Water Level Probabilities Along U.S. Coastlines. NOAA Technical Report NOS 01. National Oceanic and Atmospheric Administration, National Ocean Service, Silver Spring, MD, 111 pp. https://ocean service.noaa.gov/hazards/sealevelrise/noaa-nostechrpt01-global-regional-SLR-scenarios-US.pdf.

Tabb, D.C., D.L. Dubrow, and R.B. Manning. 1962. *The ecology of northern Florida Bay and adjacent estuaries. Technical Series no. 39*. Miami, FL: State of Florida Board Conservation.

Troxler, T.G., D.L. Childers, and C.J. Madden. 2014. Drivers of decadal-scale change in southern Everglades wetland macrophyte communities of the coastal ecotone. *Wetlands* 34: 81–90.

Van Wesenbeeck, B.K., J. Van De Koppel, P.M. Herman, M.D. Bertness, D. Van Der Wal, J.P. Bakker, and T.J. Bouma. 2008. Potential for sudden shifts in transient systems: distinguishing between local and landscape-scale processes. *Ecosystems* 11: 1133–1141.

Wang, C., and S. Temmerman. 2013. Does biogeomorphic feedback lead to abrupt shifts between alternative landscape states? An empirical study on intertidal flats and marshes. *Journal of Geophysical Research: Earth Surface* 118: 229–240.

Wang, G., X.-g. Wang, Lu, and M. Jiang. 2016. Surface elevation change and susceptibility of coastal wetlands to sea level rise in Liaohe Delta, China. Estuarine, Coastal and Shelf Science 180: 204–211.

Wang, C., L. Schepers, M.L. Kirwan, E. Belluco, A. D'Alpaos, Q. Wang, S. Yin, and S. Temmerman. 2021. Different coastal marsh sites reflect similar topographic conditions under which bare patches and vegetation recovery occur. *Earth Surface Dynamics* 9: 71–88.

Webb, E.L., D.A. Friess, K.W. Krauss, D.R. Cahoon, G.R. Guntenspergen, and J. Phelps. 2013. A global standard for monitoring coastal wetland vulnerability to accelerated sea-level rise. *Nature Climate Change* 3: 458–465.

Whelan, K.R., T.J. Smith, D.R. Cahoon, J.C. Lynch, and G.H. Anderson. 2005. Groundwater control of mangrove surface elevation: shrink and swell varies with soil depth. *Estuaries* 28: 833–843.

Wilson, B.J., S. Servais, S.P. Charles, S.E. Davis, E.E. Gaiser, J.S. Kominoski, J.H. Richards, and T.G. Troxler. 2018a. Declines in plant productivity drive carbon loss from brackish coastal wetland mesocosms exposed to saltwater intrusion. *Estuaries and Coasts* 41: 2147–2158.

Wilson, B.J., S. Servais, V. Mazzei, J.S. Kominoski, M. Hu, S.E. Davis, E. Gaiser, F. Sklar, L. Bauman, and S. Kelly. 2018b. Salinity pulses interact with seasonal dry-down to increase ecosystem carbon loss in marshes of the Florida Everglades. *Ecological Applications* 28: 2092–2108.